An Improved Real-Time Global Sea Surface Temperature Analysis

RICHARD W. REYNOLDS AND DIANE C. MARSICO

National Meteorological Center, NWS/NOAA, Washington, D.C.

(Manuscript received 2 April 1991, in final form 3 May 1992)

ABSTRACT

The monthly global sea surface temperature (SST) analysis of Reynolds using real-time in situ and satellite SST data has now been improved by using sea ice data to simulate SSTs in ice-covered regions. The simulated SSTs now become the external boundary condition for the analysis solution. This technique eliminates any high-latitude satellite biases and extends the analysis to the ice edge. The analysis with the ice data has been computed for the period January 1982 to present.

1. Introduction

A monthly real-time global sea surface temperature (SST) analysis using in situ and satellite SST data has been run at the U.S. National Meteorological Center (NMC) since 1985. This "blended" analysis has been described by Reynolds (1988). The purpose of this paper is to discuss an improvement in the technique by using sea ice data to simulate high-latitude SST data.

2. Analysis method and data

In this section we first briefly review the blending technique. We then describe the ice data and the method of adding these data to the blended analysis. All the data used here are first converted to anomalies by subtracting the monthly SST climatology of Reynolds (1988) from each observation. As described there, the climatology is based on in situ SST data (1950–79), which was augmented, in regions without in situ data, by four years of satellite SST data (1982–85) and ten years of sea ice-cover data (1973–82). The base period of the climatology thus uses data from different periods. Thus, small biases and inconsistencies in the anomalies can occur. Anomalies, however, had to be computed from the data to ensure that climatological gradients would be preserved in data-sparse regions during the blending process.

a. The blended analysis

The blended analysis uses two preliminary monthly analyses, an in situ and a satellite, as input. The in situ analysis uses quality-controlled ship and buoy SST observations obtained from the Global Telecommunication System. The monthly in situ data are averaged onto a 2-degree grid and smoothed using a nonlinear filter described in Appendix B of Reynolds (1988). The satellite analysis uses SSTs obtained from the advanced very high resolution radiometer (AVHRR) instrument using the multichannel technique of McClain et al. (1985) and Walton (1988). The satellite analysis is produced by averaging the monthly satellite SSTs onto a 2-degree grid. The most important step in the satellite analysis is a linear smoothing of the 2-degree gridded data by a two-dimensional ($\frac{1}{4}$–$\frac{1}{2}$–$\frac{1}{4}$) binomial filter.

The blending method uses the in situ analysis to define the blended field in regions of sufficient in situ observations (defined as five or more observations per 2-degree grid square). The satellite analysis is used to define the shape of the field in regions with little or no in situ data. This procedure is formally carried out by requiring that the SST field satisfy Poisson's equation. If the anomalies from the in situ analysis are defined as T, the anomalies from the satellite analysis as S, and the blended anomalies as Φ, the solution can be determined by solving

$$\nabla^2\Phi = \rho, \qquad (1)$$

where ρ is the forcing term defined below. Grid points with sufficient in situ observations define the internal boundary conditions. Thus, at these locations Φ is set equal to T. Elsewhere, (1) is solved by relaxation where the forcing term ρ is defined by

$$\rho = \nabla^2 S. \qquad (2)$$

If there are less than ten satellite observations per grid square, the satellite analysis is considered ill defined and the Laplacian $\nabla^2 S$ in (2) is locally set equal to zero. The solution of (1) automatically adjusts any large-scale biases and gradients in the satellite field rel-

Corresponding author address: Dr. Richard W. Reynolds, Coupled Model Project, NMC/NWS/NOAA, Washington, DC 20233.

ative to the in situ internal boundary conditions by use of the Laplacian operator in (2). Reynolds et al. (1989) discusses satellite biases and demonstrates that the blending technique can successfully correct them.

To obtain a well-posed solution of (1), conditions must also be defined along an external boundary that completely encloses the interior region. This is done by finding the poleward limit of the data and setting Φ equal to T or S as appropriate. If both data types are present, Φ is set equal to T. In regions where the external boundary condition is defined by the satellite field, satellite biases can enter the analysis and spread toward lower latitudes until they are eliminated by the in situ internal boundary points.

b. The blended analysis with ice data

The external boundary condition can be improved using sea-ice cover. In late 1988, real-time 2-degree gridded snow and ice fields became available on a weekly basis at NMC. These fields combined snow coverage from the National Environmental Satellite, Data and Information Service (NESDIS) and sea ice coverage from the U.S. Navy/NOAA Joint Ice Center. (The global sea ice and the Northern Hemisphere snow cover were obtained from satellite images; the Southern Hemisphere snow cover was based on NMC climatological estimates.) Grid points were considered ice covered at sea ice concentrations of 50% or greater. Because there is a permanent ice cover in the Arctic, there is always a Northern Hemisphere ice edge for every longitude; however, in the Southern Hemisphere there may be no ice edge due to lack of sea ice near the edges of the Antarctic continent in summer. To ensure a connected "ice" boundary across all longitudes, snow-covered grid points in Antarctica were treated as if they were sea ice grid points. To obtain monthly ice fields, we examined all weeks within the month and defined a grid point as ice covered if it were ice covered in at least half of the weekly fields.

Figures 1 and 2 show typical distributions of in situ, satellite, and ice-cover data for February and August. Grid points are indicated as in situ grid points if there were at least five in situ observations per month, and satellite grid points if there were at least ten satellite observations. The in situ data are shown overriding the satellite data as they do in the analysis. The figures show that the poleward data limit of in situ or satellite data is most often determined by the satellite data, particularly in the Southern Hemisphere. Thus, satellite biases can enter the blended solution via the external boundary condition. Comparison of Figs. 1 and 2 shows the seasonal shift of the data.

We use the monthly gridded ice data as follows to help bridge the gap between the poleward limit of the in situ or satellite SST data and the ice edge. The SSTs in ice-covered regions are assumed to be $-1.8°C$, the freezing point temperature of seawater with a salinity between 33 and 34 psu, which is a typical range near the ice. At these grid points, the anomalous SST, I, is defined as $-1.8°C$ minus the monthly SST climatology. The blended analysis external boundary is now defined by setting Φ equal to I at all ice-covered grid points. The solution in the interior region is unchanged. Examination of Figs. 1 and 2 shows that the use of Antarctic snow as ice ensures that the Southern Hemi-

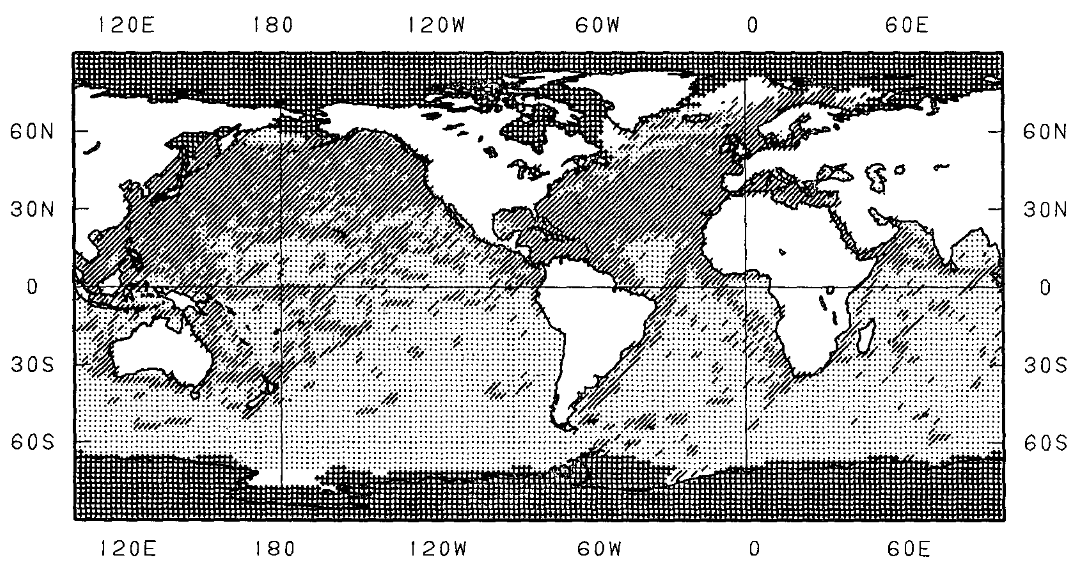

FIG. 1. Data distribution for February 1990 on a 2-degree grid. The plus (+) indicates sea ice, the solidus (/) indicates in situ data, and the dot (·) indicates satellite data. The in situ data override the satellite data; the ice data override the in situ and satellite data. Blank areas over the ocean indicate no data. The Antarctic snow-covered regions are shown as ice covered (see text).

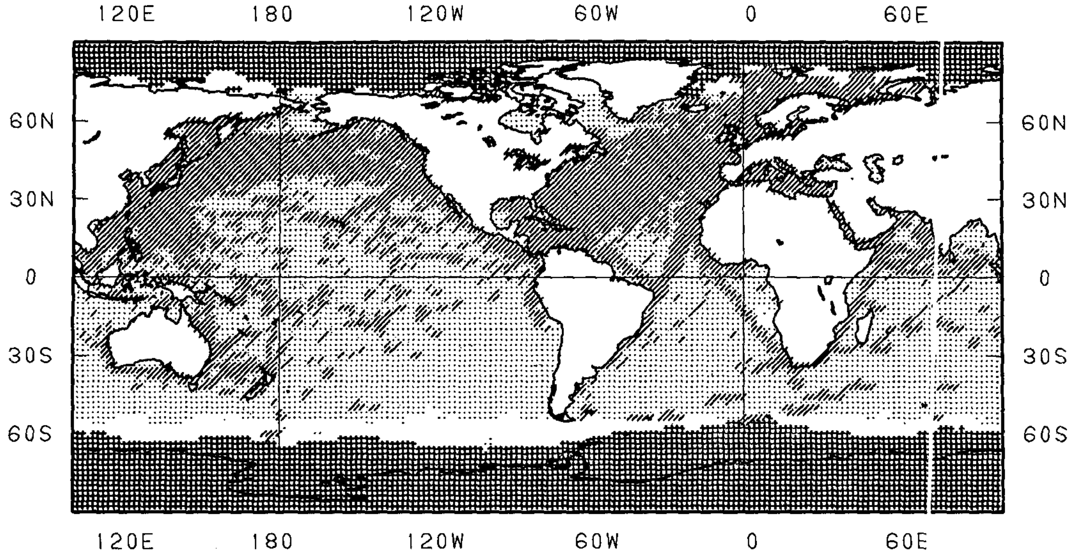

FIG. 2. As in Fig. 1 except for August 1990.

sphere external boundary conditions completely enclose the interior region. It should be noted that the blend is carried out over land. There are no SST data there except over Antarctica. Thus, the solution is determined by solving for (1) where the Laplacian $\nabla^2 S$ is zero. An anomaly can therefore extend across land. This may be reasonable because the atmosphere may force coherent SST anomalies; however, in most cases the in situ data is sufficient to define the internal boundary conditions (see Figs. 1 and 2) at the ocean and land boundaries. In the blended analysis with the ice, the satellite field is no longer needed as an external boundary condition and can only enter the solution via the Laplacian.

There is an asymmetry in these assumptions of the SST anomaly at the ice edge that depends on the relationship between the monthly and climatological ice edges. This was pointed out to us in the review process by D. Parker (U.K. Meteorological Office). When the climatological ice edge is poleward of the monthly ice edge, the anomaly at the monthly ice edge will be negative; however, when the climatological ice edge is equatorward of the monthly ice edge, the anomaly at the monthly ice edge will be zero. This would not cause a problem, if there were data adjacent to the ice edge, but this is not always the case. Ship traffic tends to avoid the navigational hazards of the ice. Satellite retrievals are not made poleward of 70° because the satellite viewing angle is too far from the satellite zenith angle for accurate retrievals. Furthermore, because satellite retrievals cannot be made in cloud covered areas, regions near the ice in the winter hemisphere may have no retrievals because of persistent cloudiness. These effects lead to the blank (no data) areas that are evident in Figs. 1 and 2 near the ice.

It is always difficult to produce an analysis where there are no data. Our method of bridging the gap between the ice and the other SST data is not perfect. In fact, as also suggested by Parker, the blending technique can permit the generation of temperatures less than −1.8°C. (This is not a unique problem for the blend but could occur in any nonlinear interpolation method.) If some assumption could be made about the SST gradient at the ice edge or the mean SST near the ice, the method could be improved; however, the SSTs near the ice can range from several degrees above freezing to freezing [Maykut and Perovich (1987) report SSTs of up to +10°C near the ice]. Furthermore, the freezing point of −1.8°C depends on the salinity, which was assumed to be between 33 and 34 psu. Because salt tends to leach out of ice, the salinity of the ice is often considerably less than 33 to 34 psu, and hence the ice has a higher melting point temperature (e.g., see Neumann and Pierson 1966).

The anomalies were adjusted so that the final temperatures were never less than −1.8°C. Because this is a lower bound on the open-ocean temperature near the ice, however, our adjustment is conservative and does not completely compensate for the asymmetry discovered by Parker. At each analysis point we define four data flags that determine what type of data was used (ice, in situ, satellite, or none.) Thus, it would be possible for the final user to reset the minimum SSTs to a value higher than −1.8°C. We did not do this because we were not certain how to define the minimum value.

Figure 3 shows the difference between the blended analysis with and without ice for August 1990. This figure illustrates that there is little difference between the analyses between roughly 50°S and 60°N, except

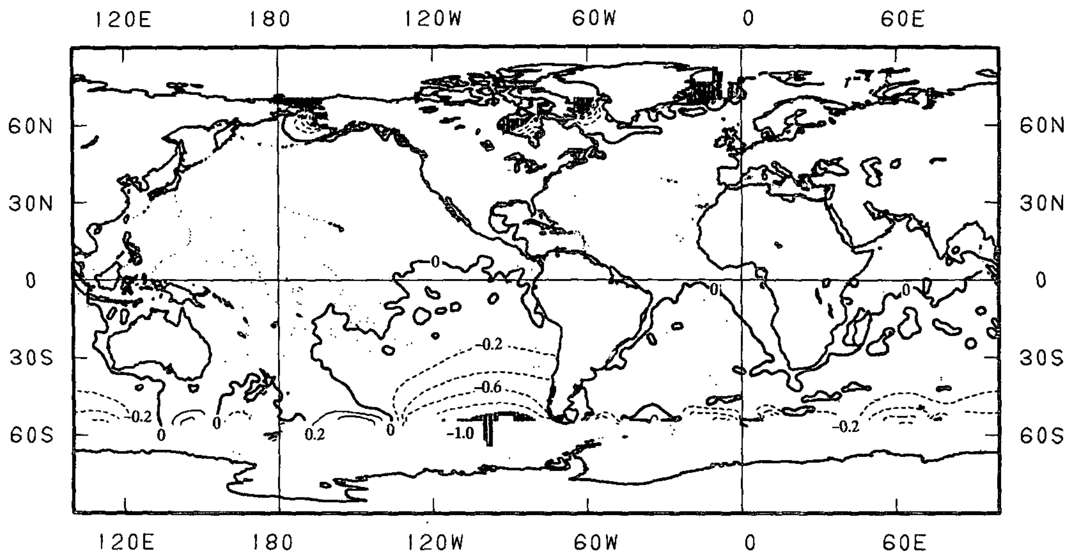

FIG. 3. Difference between analyses with and without ice for August 1990. The contour interval is 0.2°C. The heavy, solid line marks the 0° contour; the dashed lines are negative. The shaded regions indicate differences less than −1.0°C. Contours are not shown in regions beyond the poleward limit of the in situ or the satellite data.

in the eastern South Pacific. Comparison with Fig. 2 shows the differences are larger, as would be expected, in regions with sparse high-latitude in situ data. Although there are exceptions, most differences show that the analysis with the ice is colder than the analysis without the ice. Although these differences may be augmented by the asymmetries assumed at the ice boundary, there are two other possibilities, as discussed in the following.

To focus on the large differences in the eastern South Pacific, we show the zonally averaged SST anomalies between 96° and 78°W in Fig. 4. The anomalies with and without the ice are almost identical from the equator to the southern limit of the in situ data (18°S, labeled as point *A*). The two curves are not identical at 18°S because not every grid point along 18°S (see Fig. 2) is an in situ internal boundary condition. From point *A* to the southern limit of the satellite data (54°S, labeled as point *B*) the two curves diverge. Between points *A* and *B*, the shape of the satellite field is preserved by the Laplacian in both analyses. The external boundary condition, however, is set by the satellite data (point *B*) in the analysis without the ice and by the northern limit of the ice (66°S, labeled as point *C*) in the analysis with the ice. This change causes the analysis with the ice to be colder.

The ratio of the number of daytime to nighttime satellite observations suggests a qualitative reason for the bias. The global ratio during the period 1982–90 was roughly 3 to 1. This ratio was not due to a difference in day and night cloud cover but due to operational assumptions made by NESDIS. They had more confidence in their daytime cloud screening tests, which used visible information, than in the nighttime screening tests, which used infrared information. Thus, they accepted more daytime observations. The number of observations decreases at the edge of cloudy areas, such as the region designated by point *B* in Fig. 4. This decrease may completely eliminate any contribution from the sparser nighttime retrievals. Thus, the warm bias at the southern limit of the satellite data could be explained by oversampling of daytime temperatures.

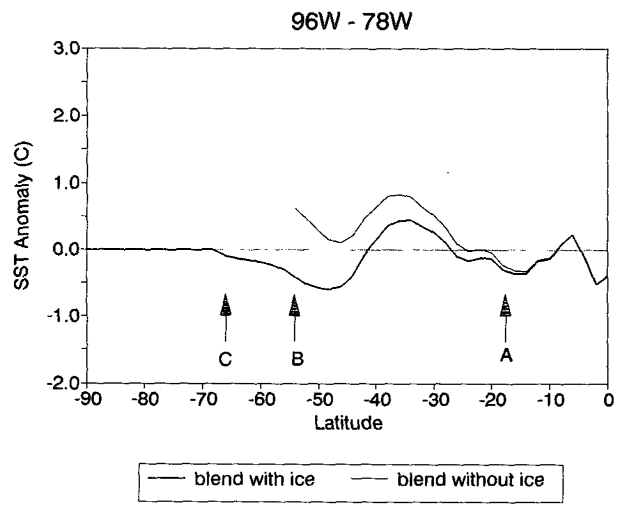

FIG. 4. Zonally averaged blended SST anomalies (in °C) for the Southern Hemisphere region between 96° and 78°W for August 1990. The light curve represents the analysis without the ice; the heavy curve represents the analysis with the ice. The "*A*" symbol indicates the southernmost limit of in situ data, the "*B*" symbol indicates the southernmost limit of satellite data, and the "*C*" symbol indicates the northernmost limit of the ice coverage. The analysis without the ice is not shown beyond the poleward limit of the satellite data.

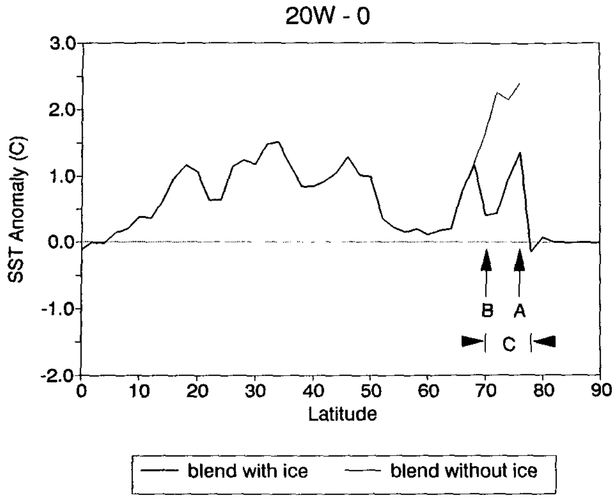

FIG. 5. Zonally averaged blended SST anomalies (in °C) for the Northern Hemisphere region between 20°W and 0° for August 1990. The light curve represents the analysis without the ice; the heavy curve represents the analysis with the ice. The "*A*" indicates the northernmost limit of in situ data; the "*B*" indicates the northernmost limit of satellite data. The "*C*" range indicates that the southernmost limit of the ice coverage varies from 70°N in the west to 78°N in the east (see Fig. 2). The analysis without the ice is not shown beyond the poleward limit of the in situ data.

Because the in situ observations were too sparse to quantitatively determine if the high-latitude Southern Hemisphere satellite data were biased, we also investigated a region in the Northern Hemisphere between 0° and 20°W, where there were more in situ data during August 1990 (see Fig. 2). There the preliminary satellite analysis was more than 0.5°C warmer than the preliminary in situ analysis between 60°N and the northern limit of the satellite data 70°N. The zonal-average difference between the blend with and without the ice is shown in Fig. 5. Here the northernmost limit of the satellite data (point *B*) is 70°N and the northernmost limit of the in situ data (point *A*) is 76°N; however, the southernmost limit of the ice ranges from 70°N in the west to 78°N in the east. Because of the density of in situ data, the satellite data have almost no impact on the external boundary condition in the analysis without the ice. The blend with the ice is colder simply due to the addition of the "ice" SST values. The blended analysis without the ice is "biased" warm in this region because it only samples open-ocean values.

We have thus identified three reasons why the blend with the ice can be systematically colder than the blend without the ice. The first is the asymmetry in the boundary assumptions at the ice edge. As mentioned above, we do not know a correction for this problem that would not potentially introduce additional errors. The second is the warm bias in satellite data that may be found near the ice edge. The blending technique with the ice data was designed to correct any satellite biases; however, the method can only correct satellite biases if there are in situ internal boundary conditions and ice external boundary conditions to determine ground truth. The third difference occurs because of the addition of SST simulated from sea-ice cover. This additional data provides a more realistic average temperature in regions near the ice edge.

3. Reanalysis

The use of ice as an external boundary condition in the blend was added to the real-time analysis starting in January 1990. The blended analysis has been computed from January 1982 to the present. (The multichannel SST retrievals became operational in November 1981. Thus, 1982 was the first complete year with these data.) We recomputed the blended analysis with the ice data for the period prior to 1990 using monthly gridded ice fields from 1982 to 1988. The 1988–89 ice fields were obtained from the weekly NMC ice fields as discussed above. The ice cover for the period 1982–87 was computed at the University of Maryland from data obtained from the World Data Center for Glaciology (Boulder, Colorado). These data were digitized from the weekly maps from the Navy/NOAA Joint Ice Center. The monthly fields were considered ice covered if monthly sea-ice concentrations were 50% or greater. The ice data in the Southern Hemisphere was also augmented by the NMC Antarctic climatological snow cover.

Figure 6 shows time series of the SST anomalies for the blended analysis with and without the ice data for the period January 1982 through December 1990 for all ocean areas between 54°S and 66°N. The analysis with the ice could be defined to the ice edge; however, the analysis without the ice was not defined beyond the poleward limit of the in situ or satellite data. Thus, the figure shows the widest latitude range for which each product could be computed. Both curves show that the past nine years have been warmer than the climatology; however, the analysis with the ice is usually slightly colder than the analysis without the ice as discussed in the preceding section.

4. Concluding remarks

The addition of SSTs simulated from sea ice cover is an important improvement in the blended analysis. This addition eliminates the need to use satellite data as an external boundary condition and allows the analysis to be defined to the ice edge. The improved analysis is thus independent of large-scale satellite biases and is defined over the entire ocean.

The principal advantage of the blending technique is an automatic correction of large-scale satellite biases and gradients relative to the in situ and ice data. The disadvantage is the loss of the higher resolution of the original satellite field. This degradation is required because the sparsity of the in situ data requires spatial

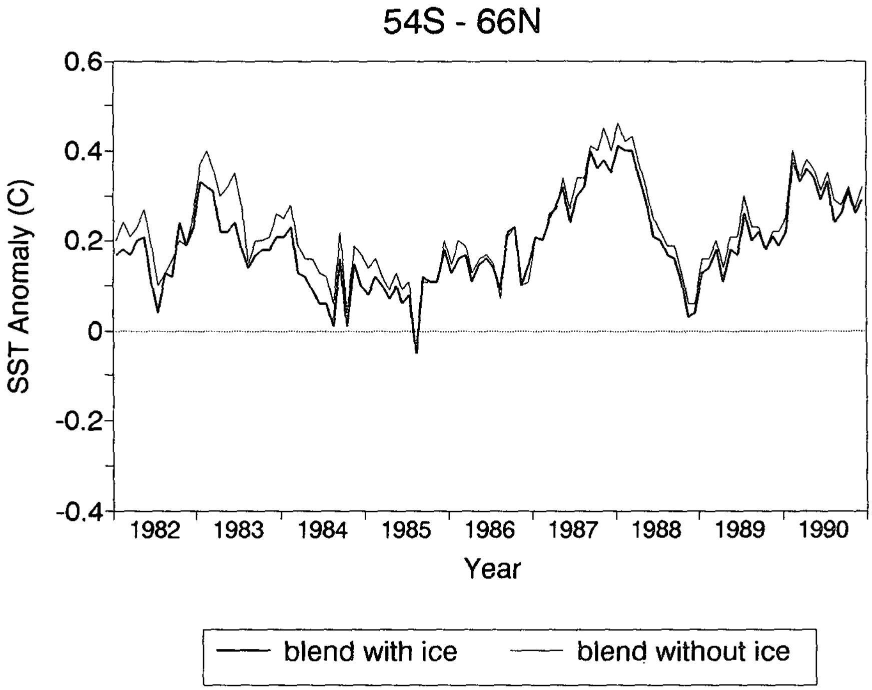

FIG. 6. Time series of the SST anomaly (in °C) for ocean areas between 54°S and 66°N for January 1982 through December 1990. The light curve represents the analysis without the ice; the heavy curve represents the analysis with the ice.

smoothing before the data can be used as the internal boundary conditions in the analysis. The present analysis method requires that both the in situ and satellite be computed on the same grid. We have developed a higher-resolution SST product using optimum interpolation (OI) following the technique of Lorenc (1981). Because the OI method assumes the data are unbiased, preliminary corrections are applied to the satellite SST data using the blending technique on a relatively coarse grid. The OI is then computed using the in situ and corrected satellite SST data on a finer grid. We will report on the OI analysis in a future article.

Acknowledgments. We are grateful to J. Shukla, D. Straus, and P. Tian of the Center for Ocean-Land-Atmosphere Interactions at the University of Maryland for producing the gridded ice fields for 1982-87 and for encouraging our reanalysis efforts. We also appreciate the editorial advice of D. Parker.

REFERENCES

Lorenc, A. C., 1981: A global three-dimensional multivariate statistical interpolation scheme. *Mon. Wea. Rev.*, **109**, 701-721.

McClain, E. P., W. G. Pichel, and C. C. Walton, 1985: Comparative performance of AVHRR-based multichannel sea surface temperatures. *J. Geophys. Res.*, **90**, 11 587-11 601.

Maykut, G. A., and D. K. Perovich, 1987: The role of shortwave radiation in the summer decay of sea ice cover. *J. Geophys. Res.*, **92**, 7032-7044.

Neumann, G., and W. J. Pierson, 1966: *Principles of Physical Oceanography.* Prentice-Hall, 545 pp.

Reynolds, R. W., 1988: A real-time global sea surface temperature analysis. *J. Climate*, **1**, 75-86.

——, C. K. Folland, and D. E. Parker, 1989: Biases in satellite derived sea-surface temperatures. *Nature*, **341**, 728-731.

Walton, C. C., 1988: Nonlinear multichannel algorithms for estimating sea surface temperature with AVHRR satellite data. *J. Appl. Meteor.*, **27**, 115-124.